Epithelial cell PPARγ contributes to normal lung maturation

Dawn M. Simon,[†] Meltem C. Arikan,[*] Sorachai Srisuma,[‡,*] Soumyaroop Bhattacharya,[*] Larry W. Tsai,[*] Edward P. Ingenito,[*] Frank Gonzalez,[§] Steven D. Shapiro,[*] and Thomas J. Mariani[*,1]

[*]Division of Pulmonary and Critical Care Medicine, Brigham and Women's Hospital, Harvard Medical School, Boston, Massachusetts, USA; [†]Division of Respiratory Diseases, Children's Hospital, Harvard Medical School, Massachusetts, USA; [‡]Department of Physiology, Faculty of Medicine Siriraj Hospital, Mahidol University, Bangkok, Thailand; and [§]Laboratory of Metabolism, National Cancer Institute, Bethesda, Maryland, USA

ABSTRACT **Peroxisome proliferator-activated receptor (PPAR)-γ is a member of the nuclear hormone receptor superfamily that can promote cellular differentiation and organ development. PPARγ expression has been reported in a number of pulmonary cell types, including inflammatory, mesenchymal, and epithelial cells. We find that PPARγ is prominently expressed in the airway epithelium in the mouse lung. In an effort to define the physiological role of PPARγ within the lung, we have ablated PPARγ using a novel line of mice capable of specifically targeting the airway epithelium. Airway epithelial cell PPARγ-targeted mice display enlarged airspaces resulting from insufficient postnatal lung maturation. The increase in airspace size is accompanied by alterations in lung physiology, including increased lung volumes and decreased tissue resistance. Genome-wide expression profiling reveals a reduction in structural extracellular matrix (ECM) gene expression in conditionally targeted mice, suggesting a disruption in epithelial-mesenchymal interactions necessary for the establishment of normal lung structure. Expression profiling of airway epithelial cells isolated from conditionally targeted mice indicates PPARγ regulates genes encoding known PPARγ targets, additional lipid metabolism enzymes, and markers of cellular differentiation. These data reveal airway epithelial cell PPARγ is necessary for normal lung structure and function.—Simon, D. M., Arikan, M. C., Srisuma, S., Bhattacharya, S., Tsai, L. W., Ingenito, E. P., Gonzalez, F., Shapiro, S. D., and Mariani, T. J. Epithelial cell PPARγ contributes to normal lung maturation. *FASEB J.* 20, E710–E720 (2006)**

Key Words: · Cre recombinase · Clara cell · lung development · airspace enlargement

PEROXISOME PROLIFERATOR-ACTIVATED RECEPTORS (PPARs) are members of the nuclear hormone receptor superfamily, which function at the transcriptional level to regulate a wide range of physiological activities. Upon activation by an appropriate ligand, PPARs form an obligate heterodimer with RXRs (cis-retinoic acid receptors) to recruit nuclear receptor coactivators to specific promoter elements, termed peroxisome proliferator response elements, and modulate gene transcription (1). There are three mammalian PPAR genes: PPARα, PPARβ/δ and PPARγ, each with unique though overlapping tissue distributions, activating ligands and regulatory activities. PPARγ is expressed in a broad range of tissues, including adipose, heart, skeletal muscle, liver, small and large intestine, kidney, pancreas, spleen, and lung (1,2). It is also expressed in a wide range of blood cells, including murine and human macrophages (3), T and B lymphocytes (4, 5) and eosinophils (6). Within the lung, PPARγ expression has been reported in the epithelium, smooth muscle, endothelium, macrophages, eosinophils, and dendritic cells. PPARγ has several naturally occurring agonists, such as polyunsaturated fatty acids and arachidonate metabolites, including hydroxyeicosatetraenoic acids (HETEs), hydroxyoctadecanoic acids (HODEs) and prostaglandin D_2 metabolite 15-deoxy-$^{\Delta 12,14}$ (15d-PGJ2). Synthetic agonists include the insulin-sensitizing agents, thiazolidinediones (TZDs) (1).

PPARγ appears to have a prominent role in regulating cellular differentiation. It is necessary and sufficient to promote the differentiation of fibroblasts into adipocytes (1,7) and within adipocytes, PPARγ regulates numerous genes involved in lipid metabolism, including adipocyte fatty acid binding protein (aP2), phosphoenolpyruvate carboxykinase (PEPCK), acyl-coenzyme A synthetase, lysosomal acid lipase 1 (Lip1) and CD36 (1). PPARγ regulates differentiation of the placental cytotrophoblast, which is necessary for placental vascularization, such that PPARγ deficiency results in embryonic death at midgestation secondary to severe cardiovascular abnormalities (8). Its role in promoting and stabilizing cellular differentiation is further evidenced by its ability to inhibit tumor cell growth *in vitro*

[1]Correspondence: Pulmonary and Critical Care Medicine, Brigham and Women's Hospital, Thorn 908, 75 Francis St., Boston, MA 02115, USA. tmariani@rics.bwh.harvard.edu

doi: 10.1096/fj.05-5410fje

0892-6638/06/0020-0710 © FASEB

and *in vivo*. PPARγ agonists have been shown to block the cell cycle, promote apoptosis, and induce differentiation of various malignant tumor cells derived from liposarcomas (9), mammary adenocarcinomas (10), lung adenocarcinomas (11), and colon cancer (12). In fact, PPARγ activation can promote the expression of markers for terminal cell differentiation in lung epithelial cell tumor lines (13, 14). Recently, PPARγ was shown to promote terminal differentiation, or "specialization", of gut epithelial cells through a mechanism involving the transcriptional coactivator Hic-5 (15).

PPARγ also has a role in the regulation of tissue inflammation in a number of organs, including the lung. PPARγ ligands can inhibit inflammatory influx and reduce airway hyperresponsiveness, airway remodeling and inflammatory cytokines in models of murine allergic hypersensitivity (6, 16). Importantly, PPARγ agonists can inhibit the expression of various inflammatory mediators from human lung epithelial cells *in vitro* (2, 6, 17). In acute lung injury models, PPARγ activation can ameliorate the inflammatory response and ultimate injury (18, 19). Some of these inflammation-related functions of PPARγ appear to be mediated, at least in part, through the ability of this transcription factor to influence states of cellular differentiation and activation. PPARγ activation can also regulate the function of various immune cells, including monocytes/macrophages (20), dendritic cells (2, 21, 22), T cells (4), and B cells (23).

PPARγ is capable of having a significant and complex influence on cellular differentiation, organ development, and the control of tissue homeostasis. On the basis of the expression pattern of PPARγ within the murine lung, we sought to understand the physiological role of epithelial cell PPARγ and its potential contribution to lung development and homeostasis. We conditionally disrupted the PPARγ gene, specifically within the conducting airway epithelium, using a novel line of transgenic mice described herein. Examination of the lungs from conditionally targeted mice reveals structural and functional abnormalities, including enlarged airspaces consistent with a deficiency in postnatal lung maturation.

MATERIALS AND METHODS

Materials and reagents

Ham's F-12 media (Cellgro, Herndon, VA, 10–080-CV); Penicillin/streptomycin (Invitrogen, Carlsbad, CA, 15140122); Gentamicin (MP Biomedicals, Aurora, OH, 16760J8); Fungizone (Invitrogen, Carlsbad, CA, 15290–018); Pronase (Roche, Indianapolis, IN, 165921); DNase I (Sigma, St. Louis, MO, DN25); FBS heat-inactivated (Invitrogen, Carlsbad, CA, 10082147); Dulbecco's modified Eagle medium/F12 (Cellgro, Herndon, VA, 15–090-CM); HEPES (Sigma, St. Louis, MO, H-4034); sodium bicarbonate (Acros Organics, Morris Plains, NJ, 217125000); L-glutamine (Invitrogen, Carlsbad, CA, 25030081); Primaria tissue culture plates (Becton Dickinson Labware, Franklin Lakes, NJ, 1353803); 10% buffered formalin (Fisher, Pittsburgh, PA, SF100–4); 4% paraformaldehyde (Electron Microscopy Sciences, Hatfield, PA, 15710); Xylene (Fisher, Pittsburgh, PA, HC700); polyclonal anti-PPARγ antibody (Ab) (Santa Cruz Biotechnology, Santa Cruz, CA, SC-6285); monoclonal anti-PPARγ Ab (Santa Cruz Biotechnology, SC-7273); anti-cytokeratin Ab (DakoCytomation, Carpinteria, CA, Z0622); anti-CC10 Ab (Santa Cruz Biotechnology, SC-9773); Harris Hematoxylin (Sigma, HHS-16); Gill's No. 3 Hematoxylin (Sigma, GHS-3–32); PBS (Fisher, Pittsburgh, PA, BP665–1); Trizol (Invitrogen, 15596–018); DNA-free (Ambion, Austin, TX, 1906); RNeasy mini kit (Qiagen, Valencia, CA, 74104); 70 micron cell strainer (Fisher, 08–771-2);

Animals

All generation and use of genetically modified animals were performed according to approved Harvard Medical School protocols. All animals were maintained in a pathogen-free barrier facility at the Harvard School of Public Health. A novel constitutive, airway epithelium specific targeting line (CCtCre) was generated using the previously described Rat 2.4 kb CC10 (also known as Clara cell secretory protein (CCSP)) promoter (24) to drive a nuclear localized form of Cre recombinase (T. Graubert and T. Ley, Washington University, St. Louis). Cre expression was confirmed using Northern blot analysis, as described previously (25). Cre function was examined by breeding with the ROSA26 Cre reporter (R26R) mouse (26), and subsequent lacZ staining was performed according to standard protocols. Briefly, offspring from these matings were sacrificed and the heart/lung isolated *en bloc* and immediately fixed in 4% paraformaldehyde for 1 h at 4°C. Fixed tissue was stained for β-galactosidase activity overnight at 30°C to avoid endogenous activity. Lung epithelium-specific PPARγ-deficient mice were generated by breeding the CCtCre transgenic line with mice harboring loxP sites flanking exon 2 of the PPARγ gene (PPARγ-floxed mice) (27). CCtCre mice were back-crossed at least 6 generations and maintained in a pure C57BL/6 background, whereas the PPARγ-floxed mice were maintained in a mixed (C57BL/6xSV129) background. The CCtCre transgenic line was bred into the PPARγ-floxed line to generate $PPAR\gamma^{floxed/wt}$, Cre^{+} mice and backcrossed to generate $PPAR\gamma^{floxed/floxed}$, Cre^{+} mice. We generated conditionally targeted and littermate controls by crossing $PPAR\gamma^{floxed/floxed}$, Cre^{+} mice with $PPAR\gamma^{floxed/floxed}$, Cre^{-} mice. Initial experiments have revealed no reduction in survival or fertility of conditionally targeted mice, facilitating this strategy. Animals were genotyped for the presence of the Cre and PPARγ-floxed alleles by tail biopsy, which provides a presumptive genotype predicting conditional targeting ($PPAR\gamma^{floxed/floxed}$, Cre^{+}) and littermate control ($PPAR\gamma^{floxed/floxed}$, Cre^{-}). Polymerase chain reaction (PCR) genotyping was performed as described previously (27). The PPARγ wild-type (WT) allele was identified at 250 bp, the floxed allele was identified at 285 bp, and Cre recombinase was identified at 350 bp. Genotypes were confirmed by postmortem analysis of lung DNA, and targeted animals were specifically defined as those displaying the recombined allele, identified at 400 bp.

Primary airway epithelial cell isolation

Tracheobronchial epithelial cells were isolated using modifications to a previously published technique (28). Briefly, 3-wk-old animals were sacrificed by CO_2 narcosis, the lungs exposed, and the tracheobronchial tree freed from the chest cavity. These were placed in Ham's F-12 media with 1× antibiotics (penicillin/streptomycin, gentamicin, and fungi-

zone) and were dissected of parenchymal tissue by securing the trachea with one forceps, whereas a sharp dissecting forceps applied gentle, continuous traction on the distal alveolar parenchyma, resulting in exposure of the tracheobronchial tree. The tissue from individual animals (n=3–5) was pooled by genotype and incubated in Ham's F-12 media with 1× antibiotics and 1.5 mg/ml pronase in 15 ml conical tubes for 18 h at 4°C. The remainder of the protocol followed the previously published technique.

Lung histology and morphometry

Conditionally targeted mice and their age-matched littermate controls were sacrificed by CO_2 narcosis. The lungs were exposed and pulmonary vasculature perfused with PBS. Three lobes of the right lung were secured individually with suture, the tissue resected and flash frozen in liquid nitrogen for RNA, protein, and DNA isolation. The left lung was inflated to a fixed pressure of 25 cm H_2O with 10% buffered formalin for 15 min. The inflated lung was removed *en bloc* and immersed in 35 ml 10% buffered formalin for 48 h at room temperature (RT) or in 4% paraformaldehyde for 24 h at 4°C. After fixation, the tissue was embedded in paraffin for histological and morphological analysis.

Slides chosen for morphometry were deparaffinized with xylene and hydrated through graded washes of ethanol. They were stained with a modified Gill's hematoxylin for 24 h: 100 ml Harris hematoxylin plus 100 ml Gill's No. 3 hematoxylin overnight at RT. The slides were washed and soaked in dilute ammonium hydroxide for 5 min then dehydrated through ethanol and washed in xylene before coverslipping. Ten random high-powered fields were captured from each sample, avoiding conducting airways, vasculature, poorly inflated regions and the pleura using MetaMorph 4.6.5 software (Molecular Devices Corp., Sunnyvale, CA). These images were then analyzed with Scion imaging (Scion Corp., Frederick, MD), measuring the linear distance between alveolar walls to compute a chord length, as well as the area of individual airspaces, to calculate the airspace area.

Microarray and quantitative real-time PCR (qPCR)

Tissue or cell pellets were homogenized in Trizol and RNA was extracted according to the manufacturer's protocol. After purification, the RNA was treated using DNA-free per manufacturer's protocol. For microarray analysis, DNA-free RNA from 2 isolates was pooled and repurified using the RNeasy mini kit. Target was generated as described previously (25) and hybridized to Affymetrix MG-U74Av2 arrays. Raw data were generated from scanned images, and signal intensities were calculated using RMA, DCHIP, and MAS5.0. Differential expression was determined using a stringent set of criteria. First, probe sets showed a consistent difference in expression (always increased or decreased) using the MAS5.0 Difference Call in all 4 pair-wise comparisons between conditionally targeted and littermate control samples. This is a nonparametric statistic that is not subject to the previously described limitations of an arbitrary fold-change threshold. Next, we calculated fold changes of all pair-wise comparisons between conditionally targeted and littermate control samples for all probe sets using RMA data. Differentially expressed probe sets were restricted to those with the 100 greatest rank sum fold changes.

Quantitative real-time PCR (qPCR) was performed essentially as described previously (29) using TaqMan chemistry. Expression analysis of lung tissue was performed by normalizing target gene expression to the endogenous control cyclophilin A, and using the mean Δ cycle threshold for the controls as a calibrator. The mean was calculated for the samples by genotype. Gene expression of the freshly isolated airway epithelial cells was analyzed by comparing the pooled conditionally targeted samples to the pooled littermate control samples, while normalizing to the endogenous control cyclophilin A. The mean expression for conditionally targeted animals was calculated as a fraction of that for littermate controls for individual experiments (n=6).

Immunochemistry

Sections of paraffin-embedded, formalin-fixed tissue were deparaffinized through xylene and hydrated through graded washes of ethanol. Immunostaining was essentially as described previously (30) using the Vectastain elite avidin-biotin complex kit (Vector Laboratories, Burlingame, CA) as per the manufacturer's instructions.

Physiology

Physiological measurements were performed essentially as described previously (31). Twelve-week-old mice were anesthetized with ketamine (75 mg/kg intraperitoneal (i.p.)) and xylazine (5 mg/kg i.p.) at doses sufficient to allow spontaneous breathing, but provide surgical-concentration anesthesia. A surgical tracheostomy was placed, and lung volumes were measured in triplicate by whole body plethysmography (BUXCO Systems, Inc., Wilmington, NC). Thereafter, additional anesthesia (1/3 original dose) was administered sufficient to suppress spontaneous respiratory efforts, and animals were placed on mechanical ventilator support (f=150 b/min, V_t=0.2 ml, 0 PEEP). Dynamic lung function (airway resistance (Raw), tissue viscance (G), and tissue elastance (H)) was assessed during forced oscillations at 0, 5, and 10 cm H_2O PEEP using a computer controlled ventilator system (SCIREQ, Inc., Montreal, Quebec). Quasi-static pressure-volume profiles (from 30 cm H_2O distending pressure to 0 cm H_2O distending pressure) were generated, and results fit to the exponential relationship $V(P) = V_{max} - Aexp(-kP)$ where P is pressure, V_{max} volume at infinite pressure, $A = V_{max} - Vmin$, Vmin = vol at 0 distending pressure, and k is the shape factor that describes the contour of the exponential pressure-volume relationship.

Statistical analysis

Two-tailed Student's t test was performed for individual comparisons between conditionally targeted and littermate control animals.

RESULTS

Spatio-temporal expression of PPARγ in the postnatal mouse lung

We used a monoclonal antibody (mAb) to investigate the cell type-specific expression pattern of PPARγ within the postnatal mouse lung (**Fig. 1**). We were unable to detect PPARγ protein before birth. Newborn

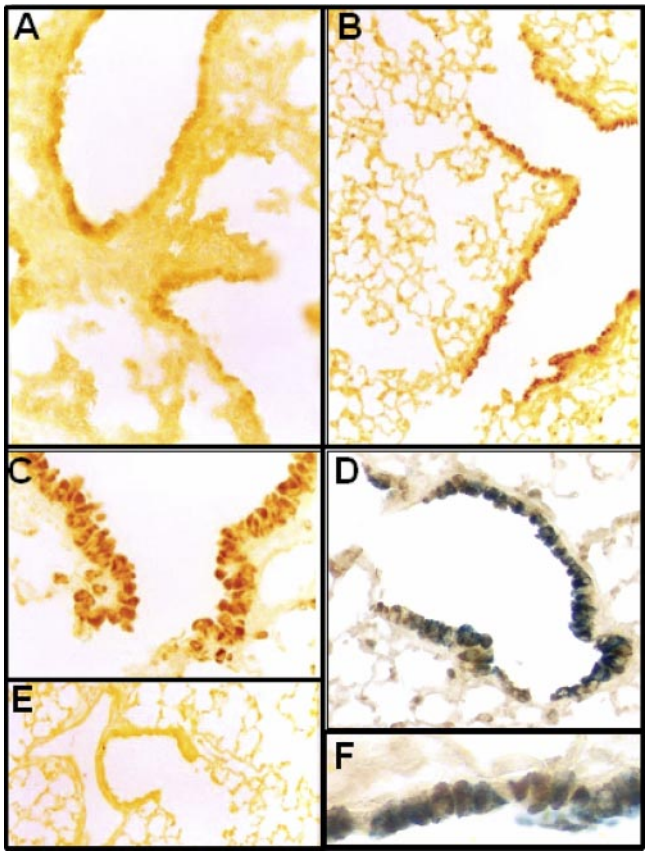

Figure 1. Localization of PPARγ expression within the airway epithelium in the mouse lung. Immunohistochemical staining using a mAb specific for PPARγ was performed to identify the temporal and cell type-specific expression of this transcription factor in the normal mouse lung. *A)* PPARγ was first detected in the newborn (1 day old) lung, as faint staining of the airway epithelium. *B)* At 4 wk of age, staining was observed within the conducting airway epithelium. *C)* Immunodetection in airway epithelial cells abruptly ends at the bronchio-alveolar duct junction. *D* and *F)* Immunohistochemistry for PPARγ (brown) and CC10 (blue) reveals colocalization for these two molecules. *E)* No staining was observed for isotype-matched, nonspecific IgG.

animals showed weak immunoreactivity, primarily within the airway epithelium (Figure 1*A*). Airway epithelial cell immunoreactivity increased throughout maturation and was evident by 4 wk of age (Figure 1*B*) and through adulthood. The proportion of PPARγ-expressing cells decreased at the proximal end of the conducting airway. At the distal end of the conducting airway, PPARγ expression was present in nearly all columnar cells and was restricted to cells at or proximal to the bronchio-alveolar duct junction (Figure 1*C*). PPARγ colocalized with CC10 but was not restricted to this population of cells (Figure 1*D*, *F*). Mature normal mouse lungs showed PPARγ reactivity in a number of nonepithelial cell types, as well (data not shown). All macrophages within the lung (as well as those obtained by lavage) showed prominent PPARγ staining. Some staining within airway and vascular smooth muscle was also observed.

Generation of targeting line

We developed a line of transgenic mice for targeting of the airway epithelium by expressing Cre recombinase under the direction of the 2.4 kb Rat CC10 promoter, as described previously (24). Over 40 founder lines were screened, and a single line was identified (CCtCre), which expressed Cre mRNA in a tissue-specific pattern restricted to the lung (data not shown). To test the efficiency for recombining loxP sites *in vivo*, we crossed the CCtCre mice with the ROSA26 Cre Reporter (R26R) mouse containing a recombination-activated lacZ transgene. These mice report tissue and cell-type specific Cre activity when appropriately stained for β-galactosidase activity (26). Newborn and 4-wk-old mice containing both the R26R allele and the Cre allele showed intense staining in the characteristic branching pattern of the airway (**Figure 2*A*, *C***). Animals containing neither transgene, or either transgene independently, showed no staining (data not shown). In histological sections (Figure 2*B*, *D*), this staining was specific to the conducting airway epithelium and not present within other cells, including the alveolar epithelium. Importantly, a relatively low concentration of recombination (20–30% of airway epithelial cells) was observed in newborn lungs, while nearly complete recombination (80–90% of airway epithelial cells) was observed at 4 wk, indicating that gene targeting mediated by this transgenic line occurs predominantly in the early postnatal period.

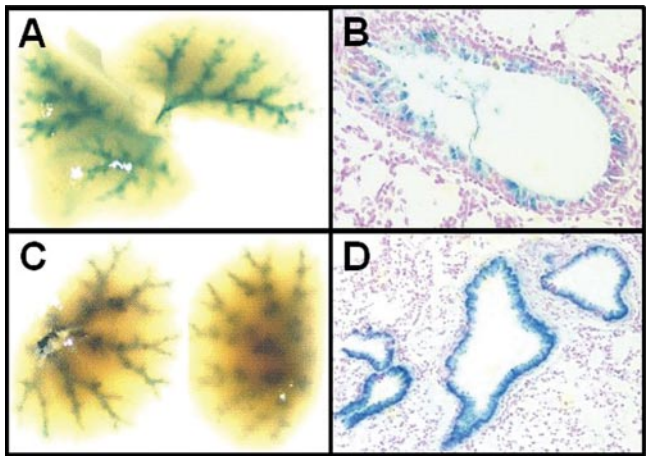

Figure 2. Airway epithelial-specific targeting in novel CCtCre line. Functional recombination activity in mice expressing Cre recombinase under control of the 2.4 kb Rat CC10 promoter was assessed using the ROSA26 Cre reporter mouse. All newborn (*A* and *B*) and mature (*C* and *D*) animals containing a copy of both transgenes showed staining within the lung. *A* and *C)* Whole mount of lungs reveal staining in the characteristic branching pattern of the airway. *B* and *D)* Histological sections show that staining is restricted to epithelial cells within the conducting airway. Further, only a minority of airway epithelial cells is stained in newborn lungs (*B*) while a majority of cells is stained in mature lungs (*D*).

Generation of airway epithelium-specific PPARγ targeted mice

The CCtCre mice described above were crossed with mice homozygous for a PPARγ allele with a pair of loxP sites flanking exon 2 of the PPARγ gene (27). Presumptive genotyping, predicting conditionally targeted ($PPAR\gamma^{floxed/floxed}$, Cre^{+}) and littermate control ($PPAR\gamma^{floxed/floxed}$, Cre^{-}) animals, was performed using isolated DNA obtained from tail biopsies. Genotypes were confirmed by analyzing lung tissue DNA for the presence of the recombined PPARγ allele, specifically within the lung. The genotypes from tail biopsy predicted the lung genotype 100% of the time.

Analysis of whole lung tissue from adult conditionally targeted mice indicated incomplete deficiency in PPARγ expression (data not shown), as expected due to the contributions of nonepithelial cells and stochastic variation in expression of the Cre transgene. To assess targeting efficiency and characterize the deficiency specifically within the epithelium, we directly assessed PPARγ expression in freshly isolated airway epithelial cells. We isolated populations of airway epithelial cells (enriched in Clara cells and ciliated cells) from conditionally targeted and littermate control mice using a modified version of a previously published method (28). Using immunocytochemistry, these isolates showed 92–93% epithelial cell purity as defined by cytokeratin immunostaining (**Figure 3*A***) and 50% Clara cells as defined by CC10 staining (Figure 3*B*). Similar epithelial cell purity and Clara cell frequency were seen among cells isolated from conditionally targeted animals and their littermate controls. PPARγ expression was assessed in the freshly isolated airway epithelial cells from conditionally targeted and littermate control mice at the steady-state mRNA and protein levels. Quantitative PCR (qPCR) revealed a 60% (P value<0.0001) reduction in PPARγ mRNA expression in airway epithelial cells derived from the conditionally targeted mice relative to controls (Figure 3*C*). Immunocytochemistry of freshly isolated airway epithelial cell cytospins with a polyclonal PPARγ Ab demonstrated a 50% reduction in the number of PPARγ expressing cells in the conditionally targeted mice when compared to littermate controls (P value<0.001) (Figure 3*D*).

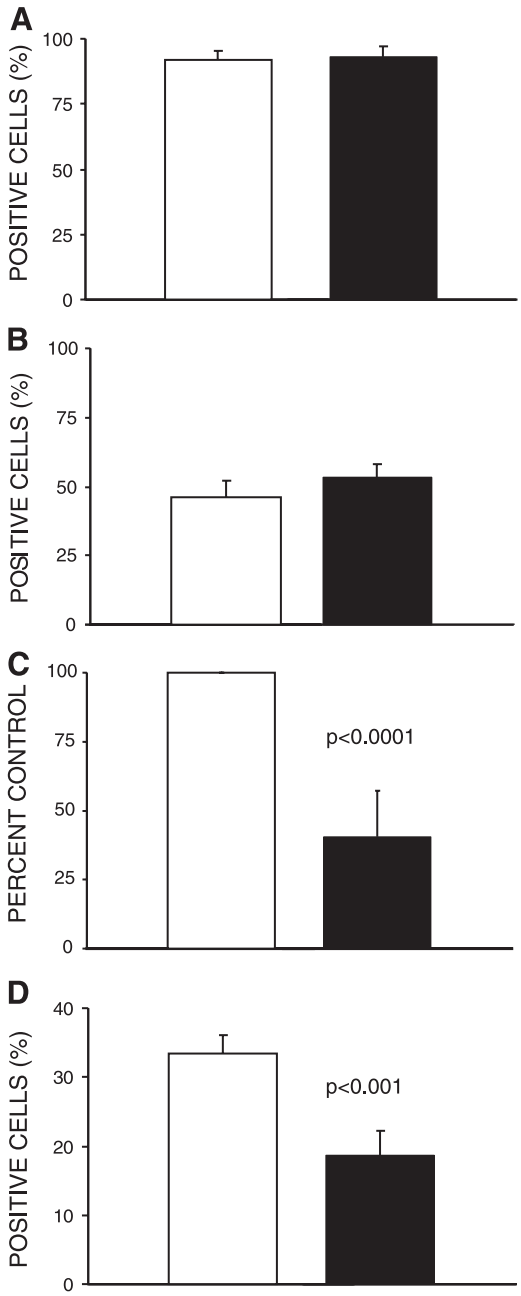

Figure 3. Characterization of PPARγ targeting efficiency. Freshly isolated primary airway epithelial cells were analyzed to define their cellular composition and PPARγ expression. *A, B)* Cytospins of airway epithelial cells stained for cytokeratin (*A*) and CC10 (*B*) for conditionally targeted animals (solid bar) and their littermate controls (open bar). *C)* qPCR using a predeveloped Taqman assay for PPARγ. Values for PPARγ mRNA expression in conditionally targeted animals were calculated relative to littermate controls for each individual experiment ($n=6$). Data are expressed as mean of the experiments ± SD. *D)* Immunostaining of cytospins using a polyclonal anti-PPARγ Ab. Data are expressed as the mean ± SD of positively stained cells ($n=4$).

Conditionally targeted mice have enlarged airspaces

Histological inspection of the lungs from adult conditionally targeted animals revealed abnormal morphology. An increase in the size of the airspaces was noted, although significant numbers of normal-appearing alveoli existed (**Figure 4*A*** and ***B***). No overt signs of inflammation or tissue destruction were observed. There were no obvious morphological changes observed in $PPAR\gamma^{floxed/wild\text{-}type}$, Cre^{+} animals (data not shown). Quantitative morphometry revealed a significant increase in airspace size in the conditionally targeted animals ($n=12$) compared with their littermate controls ($n=11$). Both the mean chord length (29.3 μm vs. 25.9 μm, P value<0.001) (Figure 4*C*) and the mean size of individual airspaces (945 μm^2 vs. 712

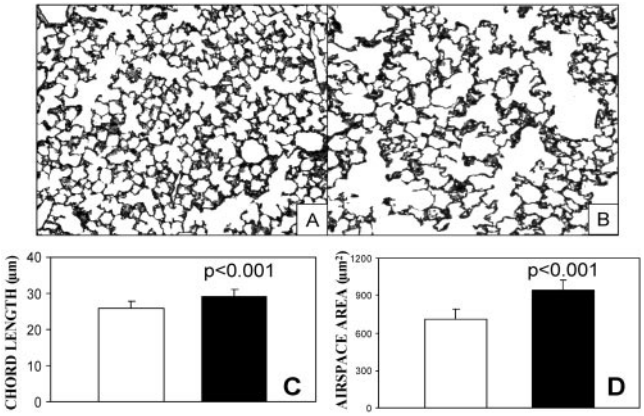

Figure 4. Morphometric analysis of lungs from 8-wk-old animals. *A, B)* Histology of lung sections stained with modified Gill's hematoxylin from 8-wk-old animals for conditionally targeted animals (*B*) and littermate controls (*A*). *C, D)* Computerized quantitative morphometric analysis of lung sections. Data are expressed as the mean chord length in micrometers (*C*) and airspace area in square micrometers (*D*) ± SD for conditionally targeted (solid bars) (n=12) and littermate control (open bars) (n=11) animals.

μm^2, P value<0.001) (Figure 4*D*) were significantly increased in conditionally targeted mice at 8 wk of age.

To define the developmental ontogeny of the phenotype, we investigated the morphology and morphometry of the lungs from younger animals (Supplemental Fig. 1). No differences were observed in either the mean chord length (28.8 μm vs. 28 μm, P value>0.5) or mean airspace area (952 μm^2 vs. 889 μm^2, P value>0.4) at 2 wk of age in the conditionally targeted animals (n=8) compared with their littermate controls (n=4). As in the adults, no signs of lung inflammation were observed in juvenile animals.

To investigate for a persistent and/or progressive nature of the phenotype, we investigated the morphology and morphometry of the lungs from aged animals (Supplemental Fig. 2). At 9 mo of age, conditionally targeted mice (n=7) showed an increase in mean chord length (10%, P value=0.07) and mean airspace area (26%, P value=0.02) (n=6) similar to that observed at 8 wk of age. Once again, no sign of a destructive phenotype was evident.

In examining the developmental ontogeny of the phenotype (**Fig. 5**), we found that the littermate control animals showed the expected reduction in airspace size coincident with completion of alveogenesis between 2 wk and 8 wk of age (7% reduction in chord length, P value=0.046 and a 20% reduction in airspace area, P value=0.002). The conditionally targeted mice did not have a reduction in airspace size during this same time (chord length increased 1.7%, P value=0.6 and airspace area decreased 0.8%, P value=0.9). During aging from 8 wk to 9 mo of age, both the littermate controls (chord length increased 5.6%, P value=0.16 and airspace area increased 14.8%, P value=0.08) and conditionally targeted animals (chord length increased 2%, P value=0.53 and airspace area increased 8.7%, P value=0.27) showed an insignificant increase in airspace size.

Conditionally targeted mice demonstrate altered lung physiology

Although airway epithelial cell PPARγ-deficient mice clearly showed a statistically significant abnormality in lung structure, the physiological consequences of this abnormality were unclear. The lung volumes of the conditionally targeted animals (n=11) and their littermate controls (n=12) were measured using whole body plethysmography, and respiratory impedance was assessed using the forced oscillation technique (**Table 1**). Tissue resistance (G) was reduced in conditionally targeted animals at normal lung volumes (4.36 $cmH_2O \cdot s^{-1} \cdot ml^{-1}$ vs. 5.86 $cmH_2O \cdot cmH_2O \cdot s/ml$, P value=0.008 at PEEP 0 cmH_2O; 4.12 $cmH_2O \cdot cmH_2O \cdot s/ml$ vs. 5.34 $cmH_2O \cdot s/ml$, P value=0.011 at PEEP 5 cmH_2O) except near total lung capacity (TLC), defined at a PEEP of 10 cmH_2O (4.9 $cmH_2O \cdot s/ml$ vs. 5.65 $cmH_2O \cdot s/ml$, P value=0.123). Though not statistically significant, dynamic elastance (H) was reduced in the targeted animals (31.48 cmH_2O/ml vs. 33.96 cmH_2O/ml, P value=0.158 at PEEP 0 cmH_2O; 22.29 cmH_2O/ml vs. 26.09 cmH_2O/ml, P value=0.075 at PEEP 5 cmH_2O; 25.18 cmH_2O/ml vs. 27.96 cmH_2O/ml, at PEEP 10 cmH_2O, P value=0.135). Additionally, in the conditionally targeted animals, there was an increase in TLC (1.16 ml vs. 0.99 ml, P value=0.017), expiratory reserve volume (ERV) (0.19 ml vs. 0.15 ml, P value=0.0007), inspiratory capacity (IC) (0.71 ml vs. 0.63 ml, P value=0.066) and vital capacity (VC) (0.9 ml vs. 0.78 ml, P value=0.016). There was no difference in airway resistance (Raw), static lung compliance (Cstat), functional residual capacity (FRC), or residual volume (RV).

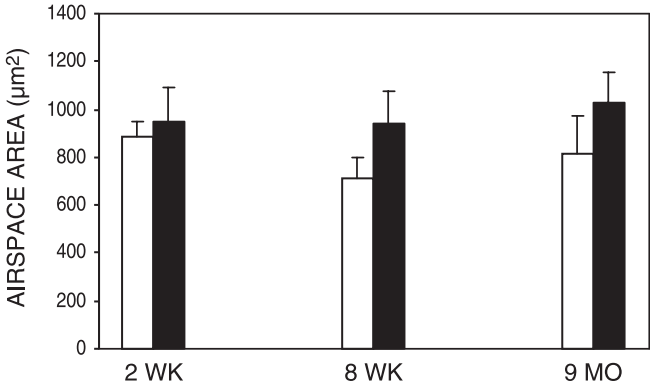

Figure 5. Developmental ontogeny of airspace enlargement. A summary of quantitative airspace morphometry during maturation (2 wk to 8 wk of age) and aging (8 wk to 9 mo of age). Data are expressed as airspace area in μm^2± SD for conditionally targeted (black bars) and control (open bars) animals. Between the ages of 2 and 8 wk, littermate control animals show a significant reduction in airspace size (P value=0.002).

Reduced ECM gene expression in the conditionally targeted animals

In order to characterize the molecular defects associated with the abnormality in lung maturation seen in the airway-specific PPARγ-targeted mice, we performed genome-wide expression profiling of lung tissue using Affymetrix U74Av2 microarrays. Whole lung tissue RNA was isolated from adult conditionally targeted and littermate control mice. RNA from two individual mice was pooled, and two separate pools from each group were analyzed. The results of these studies are presented in **Fig. 6** and Supplemental Table 1. Using highly stringent criteria, we identified 10 probe sets, representing 8 genes, most differentially expressed. Of the genes that were consistently decreased in the conditionally targeted mice, there was a dramatic overrepresentation of structural ECM genes (6 of 9 probe sets), including the elastic fiber proteins elastin (Eln) and fibrillin-1 (Fbn1) and the interstitial collagens, including procollagen type I alpha 1 (Col1a1) and procollagen type III alpha 1 (Col3a1). These findings are consistent with the observed increased airspace.

Characterization of gene expression in PPARγ-targeted airway epithelial cells

To determine the direct effects of airway epithelial cell PPARγ deficiency, we performed genome-wide expression profiling of freshly isolated airway epithelial cells from conditionally targeted and littermate control mice. The results of these studies are presented in **Fig. 7** and Supplemental Table 2. Interestingly, again there was a greater number of genes repressed (n=49) than induced (n=11) in the PPARγ-targeted cells. As anticipated, conditionally targeted airway epithelial cells showed direct effects of decreased PPARγ function. Two genes previously shown to be induced by PPARγ in other cell types, ATP-binding cassette subfamily A member 1 (Abca1) (32) and apolipoprotein E (Apoe) (33), showed significantly decreased expression. Additionally, a number of genes involved in lipid metabolism (lysosomal acid lipase 1 (Lip1), leukotriene C4 synthase (Ltc4s)) also showed decreased expression in PPARγ-targeted cells, suggesting that PPARγ plays a role in promoting normal lipid metabolism and/or homeostasis in these cells. Of particular note, a small number of genes involved in cellular differentiation (Kruppel-like factor 13 (Klf13), transforming growth factor beta 1 (Tgfb1), cathepsin B (Ctsb) and Moesin) were also dysregulated, possibly suggesting alterations in the differentiation state of these cells. Consistent with this hypothesis, PPARγ targeting resulted in dysregulation of genes previously shown to be developmentally regulated (Ctsb) (34) or differentiation-regulated (Moesin) (35) in airway epithelial cells.

TABLE 1. *Analysis of lung physiology*

	Control	Targeted	*P* value
Raw ($cmH_2O \cdot s/ml$)			
at PEEP 0	0.39	0.40	0.700
at PEEP 5	0.29	0.29	0.909
at PEEP 10	0.25	0.25	0.923
G ($cmH_2O \cdot s/ml$)			
at PEEP 0	**5.86**	**4.36**	**0.008**
at PEEP 5	**5.34**	**4.12**	**0.011**
at PEEP 10	5.65	4.9	0.123
H (cmH_2O/ml)			
at PEEP 0	33.96	31.48	0.158
at PEEP 5	26.09	22.29	0.075
at PEEP 10	27.96	25.18	0.135
Cstat (ml/cmH_20)	0.045	0.048	0.447
FRC (ml)	0.41	0.47	0.109
TLC (ml)	**0.99**	**1.16**	**0.017**
RV (ml)	0.27	0.29	0.485
ERV (ml)	**0.15**	**0.19**	**0.0007**
IC (ml)	0.63	0.71	0.066
VC (ml)	**0.78**	**0.9**	**0.016**

Invasive whole body plethysmography and mechanical ventilator support was used to investigate lung physiology for conditionally targeted animals (n=11) and littermate controls (n=12). Average measurements with *P* value derived from a two-tailed Student's *t* test are presented. Additionally, a subset of these animals (8 conditionally targeted and 8 littermate controls) had lung volume measurements performed. Measurements in bold show statistically significant values.

DISCUSSION

PPARγ is a known regulator of lung inflammation (6, 36), lung epithelial cell gene expression (2, 6, 17), and markers of lung epithelial cell differentiation (11, 13, 14). We observed a spatial and temporally restricted pattern of PPARγ expression, including prominent immunolocalization of PPARγ within the conducting airway epithelium of normal mouse lungs (Fig. 1). We hypothesized that epithelial cell PPARγ might be necessary for the establishment and maintenance of normal lung structure through regulation of epithelial cell differentiation and/or control of lung inflammation. Using a conditional targeting strategy (Fig. 2) to delete the PPARγ gene specifically within conducting airway epithelial cells (Fig. 3), we find PPARγ is necessary for normal postnatal lung maturation in mice (Figs. 4 and 5; Supplemental Figs. 1 and 2). Targeted deletion of airway epithelial PPARγ leads to a statistically significant change in lung structure at maturity, but not prior to maturity. This phenotype is persistent, but not progressive, and it occurs in the absence of overt evidence of lung inflammation or tissue destruction. To assess whether PPARγ deficiency resulted in changes in airway epithelial cell phenotypes, we assessed cell populations using immunohistochemistry for cell-specific markers. There were no apparent changes in the gross distribution of airway epithelial cells as defined by CC10 expression, or alveolar epithelial cells, as defined by SPC expression (data not shown). These data are consistent with the observed phenotype and suggest that PPARγ expression is not essential for establishment of the major classes of airway and airspace epi-

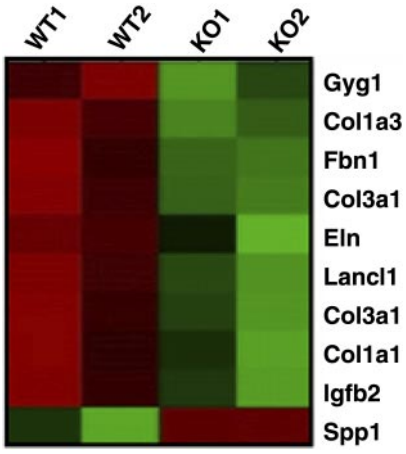

Figure 6. Gene expression profiling of whole lung tissue. Microarray analysis was performed on whole lung tissue RNA isolated from conditionally targeted (KO) and littermate control (WT) animals using the Affymetrix Mu74Av2. Shown are genes represented by probe sets, which were consistently defined as differentially expressed using stringent criteria. Columns represent individual microarray experiments, and rows indicate individual probe sets with gene identifiers. RMA-derived signal intensities are displayed in the heat plot, with green representing low expression and red representing high expression.

thelial cells, but seems to affect some characteristics of airway epithelial cell differentiation (Fig. 7).

We attempted to define the developmental ontology of the phenotype observed in the conditionally targeted mice (Fig. 5; Supplemental Figs. 1 and 2). At 2 wk of age, there was no difference in mean chord length or mean airspace area. At both 8 wk and 9 mo of age, there is an increase in mean chord length and mean airspace area from conditionally targeted mice when compared to age-matched littermate controls without evidence of inflammation. Although the littermate control animals experience the expected reduction in airspace size between 2 and 8 wk of age, coincident with alveogenesis, the conditionally targeted animals retain the same airspace size through maturation. These data suggest that the phenotype results from an insufficiency in postnatal lung maturation in conditionally targeted animals. This is not necessarily the result of a defect in alveogenesis, as numerous normal-sized alveoli exist in the conditionally targeted lungs. The precise structural nature of the airspace enlargement, whether due to alterations in alveolar or alveolar duct formation and/or structure, requires further analysis. Additionally, the degree of airspace enlargement at 9 mo is comparable to that seen at 8 wk of age. These data indicate that the abnormality in lung maturation resulting from airway epithelial cell PPARγ targeting does not lead to a progressive, destructive or inflammatory lung disease.

We were interested in determining the functional consequences of the observed abnormality. Whole body plethysmography revealed increases in the lung volumes (TLC, VC and ERV) of conditionally targeted mice and forced oscillation impedence measurements revealed alterations in lung mechanics (Table 1), particularly with respect to peripheral lung function. These physiological changes are consistent with mild airspace enlargement or emphysema.

Molecular characterization of the lungs from conditionally targeted mice using genome-wide expression profiling (Fig. 6) indicated a reduction in the expression of elastic fiber and collagen fiber components, as might be expected from the observed morphology. However, these ECM genes are expressed by mesenchymal cells and not the targeted airway epithelial cells and therefore represent a secondary effect of airway-specific PPARγ targeting. Epithelial-mesenchymal interactions are appreciated as being essential for normal lung development, primarily during embryonic growth and differentiation (37, 38). No role in postnatal matura-

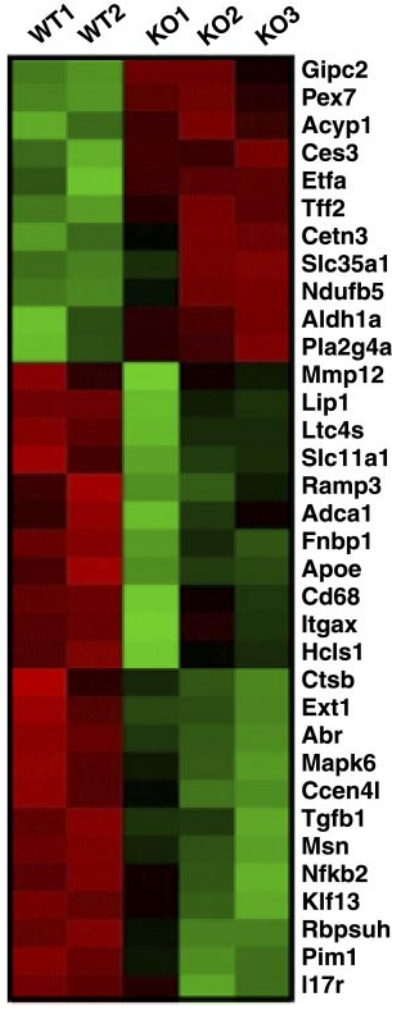

Figure 7. Gene expression profiling of isolated airway epithelial cells. Microarray analysis was performed on isolated airway epithelial cell RNA isolated from conditionally targeted (KO) and littermate control (WT) animals using the Affymetrix Mu74Av2. Shown are genes represented by probe sets, which were consistently defined as differentially expressed using stringent criteria. Columns represent individual microarray experiments, and rows indicate individual probe sets with gene identifiers. RMA-derived signal intensities are displayed in the heat plot, with green representing low expression and red representing high expression.

tion has previously been defined. The data suggest that altered epithelial-mesenchymal interactions, secondary to epithelial PPARγ deficiency, lead to changes in ECM gene expression and abnormal lung structure at maturity.

A comprehensive analysis of gene expression from purified airway epithelial cells (Fig. 7) provides insight into the physiological functions of PPARγ within this cell population. Some dysregulated genes are involved in core PPAR gene family functions, such as cellular lipid trafficking and metabolism. Some genes, including the cholesterol transporter Abca1 and the chylomicron apoprotein Apoe, have been previously shown to be PPARγ targets in other cell types (27, 33). However, these genes have no clear, previously defined role within these cells or in the lung. The fact that a number of the genes are involved in cellular differentiation (Moesin, Ctsb, Klf13) supports our conclusion that PPARγ deficiency leads to subtle alterations in airway cell phenotype that result in abnormal lung maturation. Of particular note, targeting of the gene encoding Lip1, a major neutral lipid synthesizing enzyme expressed in lung epithelial cells, results in an airspace enlargement phenotype (39). This phenotype was recently shown to be partially dependent on PPARγ inactivation (40). The Lip1-deficient phenotype is distinct from that reported here, as it involves inflammation and progressive tissue destruction. However, both of these models demonstrate a previously underappreciated, significant role for epithelial cell regulators of intracellular lipid metabolism in lung homeostasis.

PPARγ is appreciated as a physiologically relevant regulator of inflammatory responses. The particular role of epithelial cell PPARγ in contributing to these effects is not clear. We observed no evidence of inherent inflammation, nor contribution of inflammatory effects toward the phenotype of airway epithelium-specific PPARγ-targeted mice. As these animals are raised in a specific pathogen-free environment, and are never challenged with an inflammatory stimulus, we cannot conclude that airway epithelial cell PPARγ does not contribute to the regulation of inflammation in response to some stimuli. In fact, we predict that these animals will be susceptible to challenge with inflammatory stimuli, and preliminary studies have observed an increased response to chronic cigarette smoke exposure (D. Simon and T. Mariani, unpublished observations).

The novel line of Cre mice described in this report is capable of targeting loxP sites specifically within the airway epithelium with little or no recombination in other cell types during development (Fig. 2). Another important feature of this line is the predominance for recombination during late fetal and early postnatal period. Although not exogenously regulatable, this targeting allele is therefore useful to explore the functional role of genes essential for early lung development. In the mature lung, 80–90% of the airway epithelial cells are targeted (Fig. 2), with some variability between animals indicating that recombination is somewhat stochastic. It is unclear at the current time, whether this pattern is due to an early number of recombination events with subsequent proliferation to populate the majority of the airways or due to widespread recombination after birth. Interestingly, non-targeted airway cells in adult mice (as assessed in the R26R line) often occur in clusters, possibly suggesting a clonal nature of the targeted and non-targeted cells. On examination of multiple litters of conditionally targeted PPARγ mice, we find a significant and consistent ~60% reduction in airway epithelial cell PPARγ steady-state mRNA levels and a ~50% reduction in the total number of cells expressing PPARγ protein by immunostaining. The exact targeting efficiency is difficult to define, as the procedure used to isolate the airway epithelial cells results in a heterogeneous epithelial cell population, including cells where Cre recombinase and/or PPARγ are not expressed. We conclude that we have successfully targeted at minimum 50% of the PPARγ expressing airway epithelial cells. The greater than 50% reduction in steady-state mRNA levels could be due to either preferential targeting of the subset of epithelial cells expressing the highest levels of PPARγ or hemizygosity of some targeted cells or a combination of both. These data may indicate that there is a threshold concentration for PPARγ expression necessary for proper postnatal lung maturation. It is likely, however, that this threshold effect is in respect to the number of cells targeted, rather than the overall concentration of expression within the cell population or whole organ. Targeting of a greater proportion of lung epithelial cells may result in a more exaggerated phenotype.

While we targeted the airway epithelium in these mice, they developed an airspace abnormality. Although we have not determined the precise mechanisms that led to this phenotype, our data suggest that it is due (at least in part) to an alteration in epithelial cell differentiation and defect in epithelial-mesenchymal interactions. Intriguingly, Kim et al. (41) recently reported a population of lung epithelial stem/progenitor cells residing in the terminal airways, which are capable of repopulating the airspace epithelium. It is possible that our targeting involved this cell population and altered their differentiation state or stem cell potential for (re)populating the alveolus.

In conclusion, we find PPARγ is expressed within the conducting airway epithelium in mice, consistent with its localization in the airways of human asthmatics. In an effort to explore the role of this transcription factor in lung development and homeostasis, we generated a line of conditionally targeted, airway epithelial cell-deficient mice. These mice display an abnormality in postnatal lung maturation, evident as enlarged airspaces. This phenotype is persistent, but not progressive, and occurs in the absence of overt inflammation or tissue destruction. The changes in morphology are accompanied by alterations in lung physiology and whole lung ECM gene expression. Targeted airway epithelial cells show changes in gene expression con-

sistent with alterations in PPARγ function and cellular differentiation. Efforts to further define the mechanism(s) mediating this abnormality and to test the role of this transcription factor in regulating airway inflammation are the focus of current investigation. FJ

The authors would like to thank Ron McCarthy for technical assistance generating the transgenic Cre line, Chris Nicol for assistance with the floxed PPARγ mice, Jill Roby and Kathy Haley for assistance with immunohistochemistry and Jeremy Reed, Temana Andalcio and Debra Bardi for assistance with animal colony maintenance. This work was supported by Contract Grant Sponsor; NHLBI Contract Grant Number; HL071885 (T.J.M.), Contract Grant Sponsor; NHLBI Contract Grant Number; HL70321 (S.S.), Contract Grant Sponsor; American Lung Association (T.J.M.), Contract Grant Sponsor; Francis Families Foundation (T.J.M.), Contract Grant Sponsor; Cystic Fibrosis Foundation (D.S.)

REFERENCES

1. Berger, J., and Moller, D. E. (2002) The mechanisms of action of PPARs. *Annu. Rev. Med.* **53,** 409–435
2. Daynes, R. A., and Jones, D. C. (2002) Emerging roles of PPARs in inflammation and immunity. *Nat. Rev. Immunol.* **2,** 748–759
3. Chinetti, G., Griglio, S., Antonucci, M., Torra, I. P., Delerive, P., Majd, Z., Fruchart, J. C., Chapman, J., Najib, J., and Staels, B. (1998) Activation of proliferator-activated receptors alpha and gamma induces apoptosis of human monocyte-derived macrophages. *J. Biol. Chem.* **273,** 25573–25580
4. Clark, R. B., Bishop-Bailey, D., Estrada-Hernandez, T., Hla, T., Puddington, L., and Padula, S. J. (2000) The nuclear receptor PPAR gamma and immunoregulation: PPAR gamma mediates inhibition of helper T cell responses. *J. Immunol.* **164,** 1364–1371
5. Yang, L., Yan, D., Yan, C., and Du, H. (2003) PPARγ and ligands inhibit SP-B gene expression in the lung. *J. Biol. Chem.* 278: 36841–36847
6. Woerly, G., Honda, K., Loyens, M., Papin, J. P., Auwerx, J., Staels, B., Capron, M., and Dombrowicz, D. (2003) Peroxisome proliferator-activated receptors {alpha} and {gamma} down-regulate allergic inflammation and eosinophil activation. *J. Exp. Med.* **198,** 411–421
7. Zhang, J., Fu, M., Cui, T., Xiong, C., Xu, K., Zhong, W., Xiao, Y., Floyd, D., Liang, J., Li, E., Song, Q., and Chen, Y. E. (2004) Selective disruption of PPARγ2 impairs the development of adipose tissue and insulin sensitivity. *Proc. Natl. Acad. Sci. USA* **101,** 10703–10708
8. Barak, Y., Nelson, M. C., Ong, E. S., Jones, Y. Z., Ruiz-Lozano, P., Chien, K. R., Koder, A., and Evans, R. M. (1999) PPAR gamma is required for placental, cardiac, and adipose tissue development. *Mol. Cell.* **4,** 585–595
9. Tontonoz, P., Singer, S., Forman, B. M., Sarraf, P., Fletcher, J. A., Fletcher, C. D., Brun, R. P., Mueller, E., Altiok, S., Oppenheim, H., *et al.* (1997) Terminal differentiation of human liposarcoma cells induced by ligands for peroxisome proliferator-activated receptor gamma and the retinoid X receptor. *Proc. Natl. Acad. Sci. USA* **94,** 237–241
10. Mueller, E., Sarraf, P., Tontonoz, P., Evans, R. M., Martin, K. J., Zhang, M., Fletcher, C., Singer, S., and Spiegelman, B. M. (1998) Terminal differentiation of human breast cancer through PPAR gamma. *Mol. Cell* **1,** 465–470
11. Shankaranarayanan, P., and Nigam, S. (2003) IL-4 induces apoptosis in A549 lung adenocarcinoma cells: evidence for the pivotal role of 15-hydroxyeicosatetraenoic acid binding to activated peroxisome proliferator-activated receptor gamma transcription factor. *J. Immunol.* **170,** 887–894
12. Sarraf, P., Mueller, E., Jones, D., King, F. J., DeAngelo, D. J., Partridge, J. B., Holden, S. A., Chen, L. B., Singer, S., Fletcher, C., and Spiegelman, B. M. (1998) Differentiation and reversal of malignant changes in colon cancer through PPARgamma. *Nat. Med.* **4,** 1046–1052
13. Bren-Mattison, Y., Van Putten, V., Chan, D., Winn, R., Geraci, M. W., and Nemenoff, R. A. (2005) Peroxisome proliferator-activated receptor-gamma (PPAR(gamma)) inhibits tumorigenesis by reversing the undifferentiated phenotype of metastatic non-small-cell lung cancer cells (NSCLC). *Oncogene* **24,** 1412–1422
14. Chang, T. H., and Szabo, E. (2000) Induction of differentiation and apoptosis by ligands of peroxisome proliferator-activated receptor gamma in non-small cell lung cancer. *Cancer Res.* **60,** 1129–1138
15. Drori, S., Girnun, G. D., Tou, L., Szwaya, J. D., Mueller, E., Xia, K., Shivdasani, R. A., and Spiegelman, B. M. (2005) Hic-5 regulates an epithelial program mediated by PPARgamma. *Genes Dev.* **19,** 362–375
16. Honda, K., Marquillies, P., Capron, M., and Dombrowicz, D. (2004) Peroxisome proliferator-activated receptor gamma is expressed in airways and inhibits features of airway remodeling in a mouse asthma model. *J. Allergy Clin. Immunol.* **113,** 882–888
17. Wang, A. C., Dai, X., Luu, B., and Conrad, D. J. (2001) Peroxisome proliferator-activated receptor-gamma regulates airway epithelial cell activation. *Am. J. Respir. Cell Mol. Biol.* **24,** 688–693
18. Birrell, M. A., Patel, H. J., McCluskie, K., Wong, S., Leonard, T., Yacoub, M. H., and Belvisi, M. G. (2004) PPAR-gamma agonists as therapy for diseases involving airway neutrophilia. *Eur. Respir. J.* **24,** 18–23
19. Genovese, T., Cuzzocrea, S., Di Paola, R., Mazzon, E., Mastruzzo, C., Catalano, P., Sortino, M., Crimi, N., Caputi, A. P., Thiemermann, C., and Vancheri, C. (2005) Effect of rosiglitazone and 15-deoxy-delta12,14-prostaglandin J2 on bleomycin-induced lung injury. *Eur. Respir. J.* **25,** 225–234
20. Ricote, M., Li, A. C., Willson, T. M., Kelly, C. J., and Glass, C. K. (1998) The peroxisome proliferator-activated receptor-gamma is a negative regulator of macrophage activation. *Nature* **391,** 79–82
21. Gosset, P., Charbonnier, A. S., Delerive, P., Fontaine, J., Staels, B., Pestel, J., Tonnel, A. B., and Trottein, F. (2001) Peroxisome proliferator-activated receptor gamma activators affect the maturation of human monocyte-derived dendritic cells. *Eur. J. Immunol.* **31,** 2857–2865
22. Hammad, H., de Heer, H. J., Soullie, T., Angeli, V., Trottein, F., Hoogsteden, H. C., and Lambrecht, B. N. (2004) Activation of peroxisome proliferator-activated receptor-gamma in dendritic cells inhibits the development of eosinophilic airway inflammation in a mouse model of asthma. *Am. J. Pathol.* **164,** 263–271
23. Padilla, J., Kaur, K., Harris, S. G., and Phipps, R. P. (2000) PPAR-gamma-mediated regulation of normal and malignant B lineage cells. *Ann. N. Y. Acad. Sci.* **905,** 97–109
24. Hoyle, G. W., Graham, R. M., Finkelstein, J. B., Nguyen, K. P., Gozal, D., and Friedman, M. (1998) Hyperinnervation of the airways in transgenic mice overexpressing nerve growth factor. *Am. J. Respir. Cell Mol. Biol.* **18,** 149–157
25. Mariani, T. J., Reed, J. J., and Shapiro, S. D. (2002) Expression profiling of the developing mouse lung: insights into the establishment of the extracellular matrix. *Am. J. Respir. Cell Mol. Biol.* **26,** 541–548
26. Soriano, P. (1999) Generalized lacZ expression with the ROSA26 Cre reporter strain. *Nat. Genet.* **21,** 70–71
27. Akiyama, T. E., Sakai, S., Lambert, G., Nicol, C. J., Matsusue, K., Pimprale, S., Lee, Y. H., Ricote, M., Glass, C. K., Brewer, H. B., Jr., and Gonzalez, F. J. (2002) Conditional disruption of the peroxisome proliferator-activated receptor gamma gene in mice results in lowered expression of ABCA1, ABCG1, and apoE in macrophages and reduced cholesterol efflux. *Mol. Cell. Biol.* **22,** 2607–2619
28. You, Y., Richer, E. J., Huang, T., and Brody, S. L. (2002) Growth and differentiation of mouse tracheal epithelial cells: selection of a proliferative population. *Am. J. Physiol. Lung Cell Mol Physiol* **283,** L1315–L1321
29. Arikan, M. C., Shapiro, S. D., and Mariani, T. J. (2005) Induction of macrophage elastase (MMP-12) gene expression by statins. *J. Cell. Physiol.* **204,** 139–145
30. Mariani, T. J., Sandefur, S., Roby, J. D., and Pierce, R. A. (1998) Collagenase-3 induction in rat lung fibroblasts requires the combined effects of tumor necrosis factor-alpha and 12-lipoxygenase metabolites: a model of macrophage-induced, fibroblast-

driven extracellular matrix remodeling during inflammatory lung injury. *Mol. Biol. Cell* **9,** 1411–1424
31. Ito, S., Ingenito, E. P., Brewer, K. K., Black, L. D., Parameswaran, H., Lutchen, K. R., and Suki, B. (2005) Mechanics, nonlinearity, and failure strength of lung tissue in a mouse model of emphysema: possible role of collagen remodeling. *J. Appl. Physiol.* **98,** 503–511
32. Cabrero, A., Cubero, M., Llaverias, G., Jove, M., Planavila, A., Alegret, M., Sanchez, R., Laguna, J. C., and Carrera, M. V. (2003) Differential effects of peroxisome proliferator-activated receptor activators on the mRNA levels of genes involved in lipid metabolism in primary human monocyte-derived macrophages. *Metabolism* **52,** 652–657
33. Yue, L., Rasouli, N., Ranganathan, G., Kern, P. A., and Mazzone, T. (2004) Divergent effects of peroxisome proliferator-activated receptor gamma agonists and tumor necrosis factor alpha on adipocyte ApoE expression. *J. Biol. Chem.* **279,** 47626–47632
34. Buhling, F., Waldburg, N., Kruger, S., Rocken, C., Wiesner, O., Weber, E., and Welte, T. (2002) Expression of cathepsins B, H, K, L, and S during human fetal lung development. *Dev. Dyn.* **225,** 14–21
35. Tokunou, M., Niki, T., Saitoh, Y., Imamura, H., Sakamoto, M., and Hirohashi, S. (2000) Altered expression of the ERM proteins in lung adenocarcinoma. *Lab. Invest.* **80,** 1643–1650
36. Benayoun, L., Letuve, S., Druilhe, A., Boczkowski, J., Dombret, M. C., Mechighel, P., Megret, J., Leseche, G., Aubier, M., and Pretolani, M. (2001) Regulation of peroxisome proliferator-activated receptor gamma expression in human asthmatic airways: relationship with proliferation, apoptosis, and airway remodeling. *Am. J. Respir. Crit. Care Med.* **164,** 1487–1494
37. Roth-Kleiner, M., and Post, M. (2003) Genetic control of lung development. *Biol. Neonate* **84,** 83–88
38. Shannon, J. M., and Hyatt, B. A. (2004) Epithelial-mesenchymal interactions in the developing lung. *Annu. Rev. Physiol.* **66,** 625–645
39. Lian, X., Yan, C., Yang, L., Xu, Y., and Du, H. (2004) Lysosomal acid lipase deficiency causes respiratory inflammation and destruction in the lung. *Am. J. Physiol. Lung Cell Mol. Physiol.* **286,** L801–807
40. Lian, X., Yan, C., Qin, Y., Knox, L., Li, T., and Du, H. (2005) Neutral lipids and peroxisome proliferator-activated receptor-{gamma} control pulmonary gene expression and inflammation-triggered pathogenesis in lysosomal acid lipase knockout mice. *Am. J. Pathol.* **167,** 813–821
41. Kim, C. F., Jackson, E. L., Woolfenden, A. E., Lawrence, S., Babar, I., Vogel, S., Crowley, D., Bronson, R. T., and Jacks, T. (2005) Identification of bronchioalveolar stem cells in normal lung and lung cancer. *Cell* **121,** 823–835

Received for publication November 30, 2005.
Accepted for publication February 21, 2006.

Epithelial cell PPARγ contributes to normal lung maturation

Dawn M. Simon,[†] Meltem C. Arikan,[*] Sorachai Srisuma,[‡,*] Soumyaroop Bhattacharya,[*] Larry W. Tsai,[*] Edward P. Ingenito,[*] Frank Gonzalez,[§] Steven D. Shapiro,[*] and Thomas J. Mariani[*,1]

[*]Division of Pulmonary and Critical Care Medicine, Brigham and Women's Hospital, Harvard Medical School, Boston, Massachusetts, USA; [†]Division of Respiratory Diseases, Children's Hospital, Harvard Medical School, Massachusetts, USA; [‡]Department of Physiology, Faculty of Medicine Siriraj Hospital, Mahidol University, Bangkok, Thailand; and [§]Laboratory of Metabolism, National Cancer Institute, Bethesda, Maryland, USA

To read the full text of this article, go to http://www.fasebj.org/cgi/doi/10.1096/fj.05-5410fje

SPECIFIC AIMS

Peroxisome proliferator-activated receptor (PPAR)-γ has a complex influence on cellular differentiation, organ development, and the control of tissue homeostasis. This transcription factor is prominent in the conducting airway epithelium within the murine lung. We sought to understand the physiological role of epithelial cell PPARγ and its potential contribution to lung development and homeostasis by conditionally disrupting the PPARγ gene, specifically within the conducting airway epithelium, using a novel line of targeting mice.

PRINCIPAL FINDINGS

1. Generation of airway epithelium-specific PPARγ-targeted mice

Immunostaining of normal mouse lungs revealed prominent localization of PPARγ to the airway epithelium, with a majority of the staining consistent with the location of Clara cells. A novel line of mice useful for constitutive, airway epithelium-specific targeting (CCtCre) was generated using the 2.4 Rat kb CC10 promoter to drive expression of Cre recombinase. Using the ROSA26 Cre reporter (R26R) mouse, we observed airway epithelium specific targeting directed by the CCtCre transgene. Histological sections revealed targeting was specific to the conducting airway epithelium and not present within other cells, including the alveolar epithelium (**Fig. 1**). Lung epithelium-specific PPARγ-targeted mice were generated by breeding the CCtCre transgenic line with mice harboring loxP sites flanking exon 2 of the PPARγ gene (PPARγ-floxed mice). To assess targeting efficiency and characterize the deficiency specifically within the epithelium, we directly assessed PPARγ expression in freshly isolated airway epithelial cells (enriched in Clara and ciliated cells). Analysis of cells derived from the conditionally targeted mice revealed a 60% (P value<0.0001) reduction in steady-state PPARγ mRNA expression by quantitative polymerase chain reaction (PCR) and a 50% (P value<0.001) reduction in PPARγ-expressing cells by immunocytochemistry relative to littermate controls.

2. Conditionally targeted mice develop enlarged airspaces

Histological inspection of the lungs from adult conditionally targeted animals revealed abnormal morphology. An increase in the size of the airspaces was noted, although significant numbers of normal-appearing alveoli existed. No overt signs of inflammation or tissue destruction were observed. Using quantitative morphometry, we found that both the mean chord length (29.3 μm *vs.* 25.9 μm, P value<0.001) and the mean airspace area (945 μm^2 *vs.* 712 μm^2, P value<0.001) were significantly increased in conditionally targeted mice at 8 wk of age (**Fig. 2**). No differences were observed in either the mean chord length (28.8 μm *vs.* 28 μm, P value>0.5) or mean airspace area (952 μm^2 *vs.* 889 μm^2, P value>0.4) at 2 wk of age in the conditionally targeted animals compared with their littermate controls. These data indicate that the phenotype results from an insufficiency in postnatal lung maturation in conditionally targeted animals. At 9 mo of age, conditionally targeted mice showed an increase in mean chord length (10%, P value$=0.07$) and mean airspace area (26%, P value$=0.02$) similar to that observed at 8 wk of age, indicating the airspace enlargement is not progressive.

[1]Correspondence: Pulmonary and Critical Care Medicine, Brigham and Women's Hospital, Thorn 908, 75 Francis St., Boston, MA 02115, USA. E-mail: tmariani@rics.bwh.harvard.edu
doi: 10.1096/fj.05-5410fje

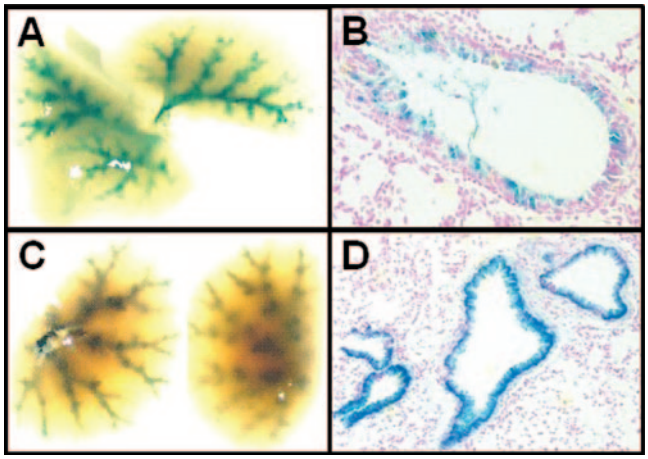

Figure 1. Airway epithelial-specific targeting in novel CCtCre line. Functional recombination activity in mice expressing Cre recombinase under control of the 2.4 kb Rat CC10 promoter was assessed using the ROSA26 Cre reporter mouse. All newborn (*A* and *B*) and mature (*C* and *D*) animals containing a copy of both transgenes showed staining within the lung. *A* and *C)* Whole mount of lungs reveal staining in the characteristic branching pattern of the airway. *B* and *D)* Histological sections show that staining is restricted to epithelial cells within the conducting airway. Further, only a minority of airway epithelial cells is stained in newborn lungs (*B*) while a majority of cells is stained in mature lungs (*D*).

3. Conditionally targeted mice demonstrate altered lung physiology

Using the forced oscillation technique, respiratory impedance demonstrated reduced tissue resistance (G) in conditionally targeted animals (4.36 $cmH_2O \cdot s/ml$ vs. 5.86 $cmH_2O \cdot s/ml$, P value=0.008 at PEEP 0 cmH_2O; 4.12 $cmH_2O \cdot s/ml$ vs. 5.34 $cmH_2O \cdot s/ml$, P value=0.011 at PEEP 5 cmH_2O), except near total lung capacity (TLC), defined at a PEEP of 10 cmH_2O (4.9 $cmH_2O \cdot s/ml$ vs. 5.65 $cmH_2O \cdot s/ml$, P value=0.123). Though not statistically significant, there was a trend toward reduced dynamic elastance and increased static lung compliance. Lung volumes were measured using whole body plethysmography and demonstrated an increase in total lung capacity (TLC) (1.16 ml vs. 0.99 ml, P value=0.017), expiratory reserve volume (ERV) (0.19 ml vs. 0.15 ml, P value=0.0007), inspiratory capacity (IC) (0.71 ml vs. 0.63 ml, P value=0.066) and vital capacity (VC) (0.9 ml vs. 0.78 ml, P value=0.016) in the targeted animals. These data are consistent with the observed airspace enlargement and confirm that the structural alterations resulting from airway epithelial cell PPARγ targeting have functional consequences.

4. Reduced extracellular matrix gene expression in the conditionally targeted animals

To characterize the molecular defects associated with the abnormality in lung maturation seen in the airway-specific PPARγ-targeted mice, we performed genome-wide expression profiling of lung tissue. Of the genes that were consistently decreased in the conditionally targeted mice, there was an overrepresentation of structural extracellular matrix (ECM) genes, including the elastic fiber proteins elastin (Eln) and fibrillin-1 (Fbn1), and the interstitial collagens, including procollagen type I alpha 1 (Col1a1) and procollagen type III alpha 1 (Col3a1). These findings are consistent with the observed increased airspace phenotype. However, as these proteins are expressed in the mesenchyme, and not by the targeted cells, they are secondary effects of airway-specific PPARγ deficiency.

5. Characterization of gene expression in PPARγ-targeted airway epithelial cells

To determine the direct effects of airway epithelial cell PPARγ deficiency, we performed genome-wide expression profiling of freshly isolated airway epithelial cells from conditionally targeted and littermate control mice. As anticipated, conditionally targeted airway epithelial cells showed direct effects of decreased PPARγ function. Two genes previously shown to be induced by PPARγ in other cell types, ATP-binding cassette subfamily A member 1 (Abca1) and apolipoprotein E (Apoe), showed significantly decreased expression in conditionally targetted cells. Additionally, genes involved in lipid metabolism (lysosomal acid lipase 1 (Lip1), leukotriene C4 synthase (Ltc4s)) also showed decreased expression in conditionally targeted cells, suggesting that PPARγ plays a role in promoting normal lipid metabolism and/or homeostasis in these cells. Of particular note, a number of genes involved in cellular differentiation (Kruppel-like factor 13 (Klf13) and transforming growth factor beta 1 (Tgfb1)) were also dysregulated in the conditionally targeted cells, suggesting alterations in the differentiation state of these cells.

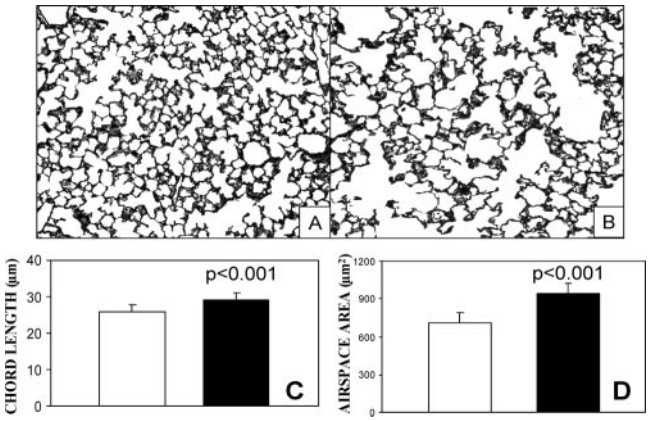

Figure 2. Morphometric analysis of lungs from 8-wk-old animals. *A* and *B)* Histology of lung sections stained with modified Gill's hematoxylin from 8-wk-old animals for conditionally targeted animals (*B*) and littermate controls (*A*). *C and D)* Computerized quantitative morphometric analysis of lung sections. Data are expressed as the mean chord length in micrometers (*C*) and airspace area in square micrometers (*D*) ± SD for conditionally targeted (solid bars) (n=12) and littermate control (open bars) (n=11) animals.

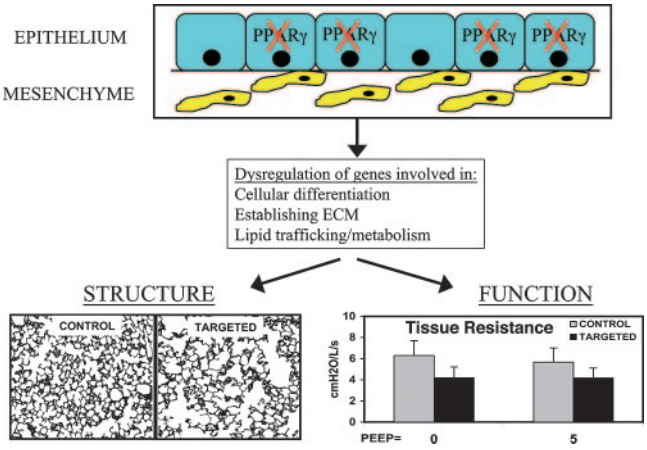

Figure 3. Schematic showing the effects of conditional disruption of airway epithelial cell PPARγ. Targeted deletion of PPARγ in the conducting airway epithelial cell results in the dysregulation of gene expression in both epithelial and mesenchymal cells. This leads to alterations in both lung structure and function in conditionally targeted animals.

CONCLUSIONS AND SIGNIFICANCE

PPARγ is a known regulator of lung inflammation, lung epithelial cell gene expression, and markers of lung epithelial cell differentiation. We hypothesized that epithelial cell PPARγ is necessary for the establishment and maintenance of normal lung structure through regulation of epithelial cell differentiation. Using a conditional targeting strategy to delete the PPARγ gene specifically within conducting airway epithelial cells, we find PPARγ is necessary for normal postnatal lung maturation. Targeted deletion of airway epithelial PPARγ leads to a statistically significant change in lung structure at maturity that is not present at 2 wk of age. Although the control animals show the expected reduction in airspace size between 2 and 8 wk of age, coincident with alveogenesis, the conditionally targeted animals retain the same airspace size through maturation. These data suggest that the phenotype results from an insufficiency in postnatal lung maturation in conditionally targeted animals. This is not necessarily the result of a defect in alveogenesis, as numerous normal-sized alveoli exist in the conditionally targeted lungs. This phenotype is not progressive with aging and occurs in the absence of overt evidence of lung inflammation or tissue destruction.

We were interested in determining the functional consequences of the observed abnormality. Whole body plethysmography revealed increases in lung volumes of conditionally targeted mice and forced oscillation impedence measurements revealed alterations in lung mechanics consistent with airspace enlargement and similar to those observed in animal models of emphysema.

Molecular characterization of lung tissue from conditionally targeted mice using genome-wide expression profiling indicated a reduction in the expression of elastic and collagen fiber components, as might be expected from the observed morphology. Epithelial-mesenchymal interactions are appreciated as being essential for normal lung development, primarily during embryonic growth and differentiation. The data suggest that altered epithelial-mesenchymal interactions, secondary to epithelial PPARγ deficiency, lead to changes in mesenchymal ECM gene expression and abnormal lung structure at maturity (**Fig. 3**). Analysis of gene expression from purified airway epithelial cells provides insight into the physiological functions of PPARγ within this cell population. Some dysregulated genes, including Lip1, are involved in core PPAR gene family functions, such as cellular lipid trafficking and metabolism. Some genes, including the cholesterol transporter Abca1 and the chylomicron apoprotein Apoe, have been previously shown to be PPARγ targets in other cell types. However, these genes have no clear, previously defined role within these cells or in the lung. The fact that a number of the genes are involved in cellular differentiation (Moesin, Ctsb, Klf13) supports our conclusion that PPARγ deficiency leads to subtle alterations in airway cell phenotype that result in abnormal lung maturation. FJ